Journal of Experimental Marine Biology and Ecology 413 (2012) 60–70

Contents lists available at SciVerse ScienceDirect

Journal of Experimental Marine Biology and Ecology

journal homepage: www.elsevier.com/locate/jembe

Robotic sampling, in situ monitoring and molecular detection of marine zooplankton

Julio B.J. Harvey *, John P. Ryan, Roman Marin III, Christina M. Preston, Nilo Alvarado, Chris A. Scholin, Robert C. Vrijenhoek

Monterey Bay Aquarium Research Institute, 7700 Sandholdt Rd, Moss Landing, California 95039, USA

ARTICLE INFO

Article history:
Received 10 November 2011
Received in revised form 22 November 2011
Accepted 23 November 2011
Available online 21 December 2011

Keywords:
18S ribosomal RNA probes
Autonomous Underwater Vehicle
Copepods
Environmental Sample Processor
Invertebrate larvae
Upwelling

ABSTRACT

Recent advances in robotic technologies provide new opportunities to conduct high-resolution sampling of patchily distributed zooplankton and associated environmental variables. We used two robots and molecular probes to assess the temporal and spatial variability of zooplankton in water samples obtained from Monterey Bay, California. The Autonomous Underwater Vehicle (AUV) *Dorado* is a mobile platform that carries ten, 1.8-L bottles ("Gulpers") capable of rapidly acquiring discrete seawater samples, and an extensive sensor suite for gathering contextual environmental data during day-long expeditions. Molecular assays were conducted ex situ at a shore-based laboratory. In contrast, the Environmental Sample Processor (ESP) was deployed as a stationary (moored) device capable of repeatedly "sipping" water to conduct in situ molecular assays and record environmental data during month-long deployments. Molecular analyses were conducted with the sandwich hybridization assay (SHA), which employed 18S ribosomal RNA oligonucleotide probes designed to detect calanoid and podoplean copepods, and the larvae of barnacles, mussels, polychaete worms, brachyuran crabs, and invasive green crabs (*Carcinus maenas*). Both the stationary and mobile sampling protocols revealed the greatest zooplankton diversity and abundance in relatively warm waters, higher in chlorophyll and lower in salinity and nitrate. Diversity and abundance were least in recently upwelled waters with the inverse conditions. High-resolution sampling revealed that while calanoid copepods were generally associated with elevated chlorophyll, they were most abundant in upwelling fronts, in some cases. These narrow features appear to provide favorable conditions for the growth and aggregation of certain zooplankton.

1. Introduction

Hutchinson (1961) identified the spatial patchiness and temporal variability of aquatic ecosystems as one way to explain the paradox of plankton diversity. Consequently, marine biologists strive to accurately assess widely variable zooplankton diversity and abundance at a variety of spatial scales from coastal regions to ocean-basins (e.g., Bucklin et al., 1995; Scheltema, 1986; Thorson, 1950). Traditional sampling methods (e.g., vertical and horizontal tow nets and bottle samplers) provide fundamental insights into the distribution and abundance of zooplankton species that support fisheries and healthy marine ecosystems (e.g., Keister et al., 2009a; Mackas and Beaugrand, 2010; McClatchie et al., 2008; Puig et al., 2001), but these methods homogenize (smear) small-scale spatial heterogeneity across the length of a sample trajectory. Bottle-samplers (e.g., Niskin rosettes) actuated at fixed depths and locations can accurately sample at smaller scales, but they have a high probability of missing mobile patches of aggregated zooplankton. The Hardy continuous plankton recorder (Reid et al., 2003) can sample patchiness along a tow trajectory. However, this system was designed to cover large spatial scales at low spatial resolution and is therefore not well suited for studying small-scale patchiness. Finally, deriving qualitative and quantitative information about zooplankton composition from all of these methods requires time- and labor-intensive microscopic examinations and taxonomic analyses. Molecular systematic methods can potentially accelerate post-sampling identification of zooplankton (reviewed in Darling and Blum, 2007; Garland and Zimmer, 2002), but to date most of these studies have been proof-of-concept in scope (e.g., Harvey et al., 2009; Jones et al., 2008; Patil et al., 2005).

To augment studies of plankton patchiness and ecology, the Monterey Bay Aquarium Research Institute (MBARI) has developed robotic technologies with advanced water-sampling capabilities and concurrent acquisition of contextual environmental data at high spatial and temporal resolution. These technologies differ in the ways they sample water in space and time. Spatial sampling is accomplished with the Autonomous Underwater Vehicle (AUV) *Dorado*, a mobile platform programmed to obtain water samples at specified geographical locations and depths. The AUV is equipped with ten, 1.8-L bottles ("Gulpers", Bird et al., 2007) that rapidly acquire individual samples for subsequent ex situ molecular analyses (Ryan et al., 2010). In contrast, the Environmental Sample Processor (ESP) is typically deployed in a stationary mode, attached to a mooring and

* Corresponding author. Tel.: +1 831 775 1789; fax: +1 831 775 1620.
E-mail address: jharvey@mbari.org (J.B.J. Harvey).

0022-0981/$ – see front matter © 2011 Elsevier B.V. All rights reserved.
doi:10.1016/j.jembe.2011.11.022

programmed to sample temporally for periods up to 30 days. Second-generation ESP devices use in situ, microarray-based, molecular methods to analyze water samples in near real-time (Jones et al., 2008; Preston et al., 2011; Scholin et al., 2009). The ESP slowly acquires ('sips') its water volumes (≤4 L) during a 30–60 min sampling period. Both sampling systems include an integrated suite of environmental sensors so that physical, chemical and optical conditions are measured throughout the deployment, including conditions directly coincident with sample acquisition.

Compared to tow nets, these robotic technologies sample very small volumes of water; consequently, organisms that are present in low abundance might not be collected, except in a random, Poisson-distributed, fashion. Also, the rapid gulping and slow sipping methods are expected to exhibit sampling biases for organisms with different reaction capabilities and escape velocities. Nonetheless, when integrated with molecular probes, the ESP and AUV/Gulper methods have demonstrated their abilities to detect the presence and abundance of common phytoplankton, invertebrate larvae, and bacteria in small water samples (Goffredi et al., 2006; Preston et al., 2009; Ryan et al., 2010). Molecular identification of these organisms uses the sandwich hybridization assay (SHA), well recognized for its repeatability and robustness in detecting target organisms from biologically complex water samples (Greenfield et al., 2006; Haywood et al., 2007; Smith et al., 2011). Integration of robotic sampling and molecular identification methods has demonstrated their capacity to detect fine-scale variations in the abundance of common zooplankton such as the taxa associated with intermediate nepheloid layers in Monterey Bay, California (Ryan et al., 2010).

Here, we report the use of ESP and AUV/Gulper technologies to detect marine invertebrate larvae and major copepod groups in seawater samples associated with different water types and associated upwelling fronts in Monterey Bay, California. Contextual environmental data were obtained from multiple deployments involving both platforms during 2009. Previously developed SHA probes were used to detect various invertebrate larvae (Goffredi et al., 2006; Jones et al., 2008). We designed new probes to detect calanoid and podoplean copepods, and brachyuran crabs. Our specific goals were to assess: (1) the spatial and temporal variables associated with patchiness in zooplankton biodiversity and abundance; (2) the relative merits of stationary versus mobile sampling platforms; and (3) the environmental features that provide suitable targets for subsequent hypothesis testing with adaptive sampling protocols.

2. Methods

2.1. AUV/Gulper samples

We conducted nine deployments in Monterey Bay, California (e.g., Fig. 1) between 25 March and 30 June 2009 (Table 1). Each deployment collected up to ten discrete ~1.8 L seawater samples (Bird et al., 2007; Ryan et al., 2010). Rapid intake (gulps taking 1 to 2 s) ensured acquisition of discrete samples. Autonomous control software triggered sample acquisition at prescribed depths and geographic locations. Location data were simultaneously recorded with corresponding measurements of temperature, salinity, optical backscattering, and concentrations of nitrate, oxygen, and fluorometric chlorophyll-a (Ryan et al., 2008).

Upon recovery of the vehicle, samples were vacuum filtered (described in Ryan et al., 2010) onto three or four, 5 μm Durapore filters (Millipore, Billerica, Massachusetts). Samples were equally apportioned among individual filters and stored in 2-mL cryogenic vials in liquid nitrogen. Lysis of the samples (described by Jones et al., 2008) and lysate filtration were conducted with 0.22 μm Millex-GV, 33 mm syringe filters (Millipore). The laboratory-based, 96-well plate version of SHA was used to analyze AUV water samples (described by Goffredi et al., 2006).

Statistical analyses were conducted with PRIMER version 6.1.6 (PRIMER-E, Plymouth, United Kingdom). Environmental variables were normalized (Mean divided by the Standard Deviation) prior to Principal Components Analysis (PCA) of the correlation matrix. A resemblance matrix of Euclidean distances was generated to conduct cluster analysis via group average, single and complete linkage clustering modes for comparison to PCA. Biological signal detection from each sample was then compared to PCA scatter plots. Oceanographic data associated with samples were examined graphically within SIGMAPLOT 2002 version 8.02 (Systat Software Inc., San Jose, CA).

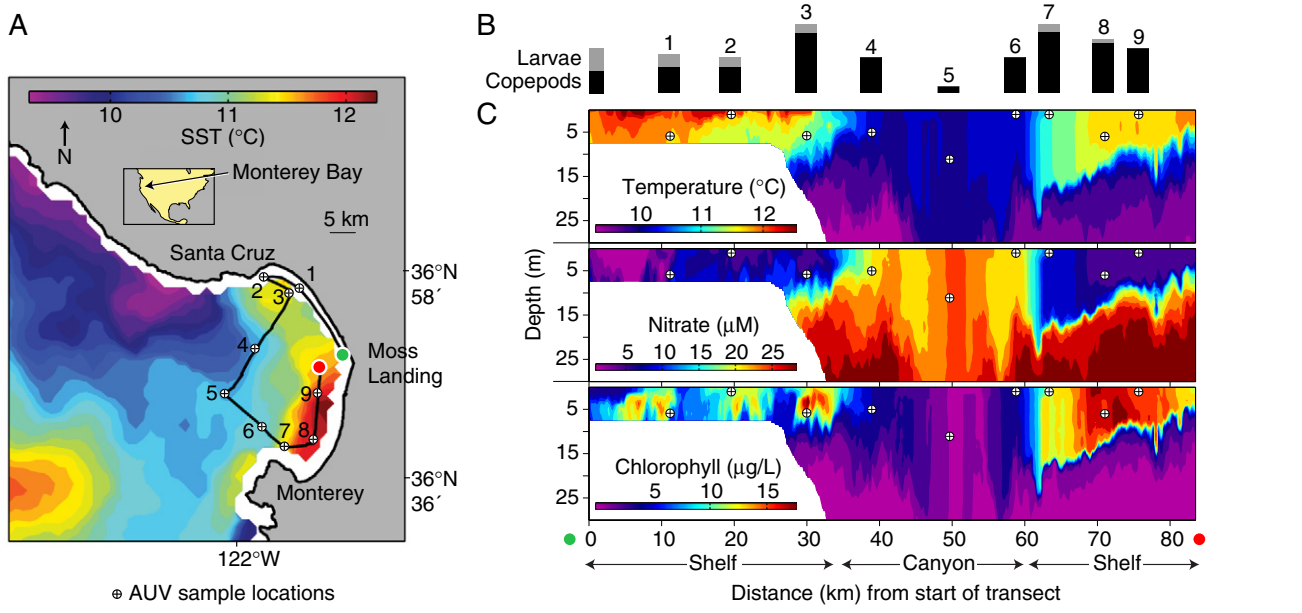

Fig. 1. One AUV survey of Monterey Bay, 25 March 2009. (A) Map of sea-surface temperatures (SST) with AUV track and locations of the nine water samples collected. Green and red dots indicate AUV deployment and recovery locations respectively. White area indicates the absence of SST data. (B) Zooplankton probe signals (A450 nm OD) combined for invertebrate larvae (gray bars = barnacle + mussel + polychaete + *C. maenas* + brachyurans) and combined copepods (black bars = calanoid + podoplean) for each of the AUV water samples. (C) Synoptic maps for temperature, nitrate and chlorophyll along the survey track. Water sample locations are indicated. White areas indicate the bottom plus a 5–7 m buffer maintained by the AUV.

Table 1
AUV/Gulper samples and SHA signal detection for larval and copepod probes. Deployment dates in 2009 are given with depths and coordinates of samples. Dashes (–) signify no target detection above background signal. Probe targets: Cal1939 for calanoid copepods; Pod1951 for podoplean copepods; Cal 903 for calanoid copepods; B1006 for barnacles; M2B for mussels; P1022 for polychaetes; Crab903 for brachyuran crabs; GCRAB for *Carcinus maenas*.

Date	Sample	N Lat.	W Lon.	Depth (m)	Cal1939	Pod1951	Cal903	B1006	M2B	P1022	Crab903	GCRAB
25 Mar	1	36.9097	238.1355	6.4	0.479	0.110	0.122	0.127	0.104	–	0.105	–
	2	36.9561	238.0662	0.0	0.701	–	–	0.118	0.155	–	–	–
	3	36.9000	238.0854	5.4	1.539	–	–	0.108	0.120	–	–	–
	4	36.8310	238.0378	5.0	0.889	–	–	–	–	–	–	–
	5	36.7509	237.9844	11.1	0.114	–	–	–	–	–	–	–
	6	36.6912	238.0536	0.0	0.889	–	–	–	–	–	–	–
	7	36.6600	238.0881	1.1	1.406	0.156	0.103	0.108	–	–	–	–
	8	36.6932	238.1424	6.3	1.030	0.184	0.136	–	0.111	–	–	–
	9	36.7349	238.1460	0.0	0.957	0.129	0.113	–	–	–	–	–
26 Mar	10	36.8268	238.0945	10.7	0.755	–	0.106	0.106	–	–	–	–
	11	36.8393	238.0993	10.1	0.422	–	0.108	–	–	–	–	0.102
	12	36.8260	238.0963	11.2	0.437	–	0.114	–	–	–	–	–
	13	36.8391	238.0995	11.3	0.358	0.109	–	–	–	–	–	–
	14	36.8260	238.0967	10.9	0.412	–	–	–	–	–	0.123	–
	15	36.8391	238.0992	11.0	0.753	0.106	0.113	–	–	–	–	–
21 Apr	16	36.8853	238.1031	5.6	0.780	0.147	0.132	–	0.112	0.100	–	–
	17	36.8723	238.1037	5.7	1.722	0.110	0.116	–	–	–	–	–
	18	36.8624	238.1028	5.9	0.484	0.111	–	–	–	–	–	–
	19	36.8508	238.1034	5.8	1.380	0.119	–	0.114	0.113	–	–	–
	20	36.8413	238.1035	5.1	2.938	0.114	–	–	–	–	–	–
	21	36.8336	238.1018	5.5	0.644	–	–	–	–	–	–	–
	22	36.8252	238.1016	5.9	0.981	0.118	0.139	–	–	–	–	–
	23	36.8083	238.1045	6.0	0.352	–	–	–	–	–	–	–
	24	36.7907	238.1058	6.1	0.254	0.113	–	–	–	–	–	–
	25	36.7738	238.1046	4.2	0.365	–	–	0.243	0.114	–	–	–
22 Apr	26	36.8851	238.1011	6.0	2.730	0.172	0.142	0.112	0.104	–	–	–
	27	36.8727	238.1034	5.0	1.843	0.257	0.144	–	–	–	–	–
	28	36.8620	238.1033	5.9	1.811	0.170	–	–	–	–	–	–
	29	36.8514	238.1034	6.1	1.041	–	–	0.184	–	–	–	–
	30	36.8413	238.1037	6.0	0.775	0.108	–	–	–	–	–	–
	31	36.8338	238.1017	5.0	1.240	0.131	–	–	–	–	–	–
	32	36.8254	238.1018	5.9	3.480	0.254	0.169	–	–	–	–	–
	33	36.8079	238.1050	5.0	2.939	0.353	0.117	–	–	–	–	–
	34	36.7908	238.1056	4.6	2.492	0.354	0.108	–	–	–	–	–
	35	36.7745	238.1050	4.4	2.201	0.175	0.130	–	–	–	–	–
23 Apr	36	36.8843	238.1011	5.0	1.809	0.169	0.128	–	0.103	–	–	–
	37	36.8719	238.1034	5.0	1.577	0.137	–	–	–	–	–	–
	38	36.8608	238.1032	5.9	2.741	0.142	0.138	–	–	–	–	–
	39	36.8495	238.1032	5.3	1.823	0.131	–	0.101	–	–	–	–
	40	36.8410	238.1024	5.8	1.257	–	–	–	–	–	–	–
	41	36.8326	238.1011	4.8	1.120	–	–	–	–	–	–	–
4 May	42	36.8478	238.1765	6.1	0.600	0.203	–	–	–	–	–	0.110
	43	36.9094	238.1356	6.1	1.631	0.314	0.115	0.125	–	–	–	–
	44	36.9565	238.0659	6.0	0.887	0.228	0.133	0.107	0.121	0.108	–	–
	45	36.8983	238.0866	6.1	1.140	0.238	–	–	–	–	–	–
	46	36.8320	238.0390	5.1	0.196	–	–	–	–	–	–	–
	47	36.7535	237.9858	5.6	0.318	0.233	–	–	–	–	–	–
	48	36.6919	238.0565	5.8	0.229	–	–	–	–	–	–	–
	49	36.6597	238.0901	6.1	0.372	–	–	–	–	–	–	–
	50	36.6926	238.1417	5.7	1.321	0.142	0.103	–	–	–	–	–
	51	36.7345	238.1455	5.8	0.256	–	–	–	–	–	–	–
1 Jun	52	36.8214	238.0870	5.5	0.163	0.100	–	–	–	–	–	–
	53	36.8312	238.0989	6.5	0.571	0.181	0.115	–	0.138	0.120	–	–
	54	36.8421	238.1115	6.1	0.626	0.415	0.135	–	0.136	–	–	–
2 Jun	55	36.8233	238.1143	7.0	0.255	0.162	–	–	0.174	–	–	–
	56	36.8212	238.0876	6.9	0.512	0.184	–	–	0.176	–	–	–
	57	36.8312	238.0993	6.9	0.358	0.181	–	–	–	–	–	–
	58	36.8416	238.1117	6.6	0.267	0.299	–	0.198	–	–	–	–
30 Jun	59	36.8881	238.0654	13.1	0.175	0.102	–	0.117	0.149	–	–	–
	60	36.8845	238.0611	12.7	0.136	–	–	0.111	0.148	–	–	–
	61	36.8845	238.0610	13.0	0.287	–	–	–	–	–	–	–
	62	36.8845	238.0610	13.4	0.261	0.220	–	–	–	–	–	–

2.2. ESP samples

In 2009, samples were collected during three, month-long deployments in Monterey Bay. Because deployed ESPs ran multiple experiments, the in situ analyses of zooplankton samples were conducted during the following time periods: Spring (20–22 April); Fall-1 (29 September–7 October) and Fall-2 (15–16 October). The spring deployment occurred at MBARI's M0 mooring (N Lat 36.8337, W Lon 121.8986) and the fall deployments occurred in the Santa Cruz Bight (Fall-1: N Lat 36.9272, W Lon 121.9734; Fall-2: N Lat 36.9000, W Lon 121.8820). Control software and mechanical details of second-generation (2G) ESP technology were previously described (Greenfield et al., 2006; Roman et al., 2007; Scholin et al., 2009). Each water sample (up to 4 L) was passed through a high volume "puck" to collect organisms on a custom 25 mm, 10 μm porous titanium frit (Chand Eisenmann Metallurgical, Burlington, Connecticut),

rather than a filter membrane. After sample lysis, the ESP applied each sample lysate to a microarray composed of oligonucleotide SHA capture probes. Complete SHA microarray methods developed for the ESP are well documented (Greenfield et al., 2006; Jones et al., 2008; Preston et al., 2009). Results of molecular probing were visualized with the ESP IMAGE ANALYSIS APPLICATION (Schlining, 2009) and IMAGE J software (Rasband, 2008). Temperature, salinity, depth, turbidity, and chlorophyll-a data were averaged across sample collection intervals of 1–2 h. Graphical methods were used to assess the correspondence between SHA signals and environmental variables.

2.3. SHA probes

Previously developed signal probes (Euk519, Euk915, and Euk1194) and capture probes were used to detect invertebrate larvae: B1066 for barnacles, M2B for mussels, P1022 for polychaetes, GCRAB for *C. maenas*, and Euk338 for eukaryotes (Goffredi et al., 2006; Jones et al., 2008). To detect specific copepod groups and brachyuran crabs, we designed four new capture probes to function with the aforementioned signal probes (Table 2). Annealing sites were selected from hyper-variable regions to exclude taxa with one or more nucleotide base-pair mismatches. For example, Cal903 was designed to exclude non-calanoids. Additionally, some members of the calanoida were also excluded (e.g., *Pseudocyclops* sp. through *Acartia tonsa*, Table 2). Subsequent efforts will focus on designing more specific probes to detect these calanoids. Cal903 and Cal1939 were designed to detect different subsets of calanoid taxa. Pod1951 was designed to detect the following orders in the superorder Podoplea: Cyclopoida, Siphonostomatoida, Poecilostomatoida and Harpacticoida. Crab903 was designed to detect brachyuran crabs and discriminate against other crustacean orders. New SHA capture probes were designed to anneal 100 to 300 base-pairs (bp) distant from signal probe sites. General methods for probe design are documented elsewhere (Harvey et al., 2009). We used the SEQUENCE MANIPULATION SUITE (Stothard, 2000) to determine homodimer and stem loop formation potential for each probe. Capture probes synthesized by Oligos, Etc. (Wilsonville, OR) had a 5′-biotin label separated from the coding sequence by a non-reactive spacer region, nine carbons in length (C9 spacer). SHA reagents and methods for both 96-well plate (Goffredi et al., 2006; Scholin et al., 1999) and microarray versions (Greenfield et al., 2008; Jones et al., 2008; Preston et al., 2011) are documented elsewhere. Briefly, 1.5 mol L^{-1} GuSCN lysis buffer was applied to filter collected samples with 85 °C heating. Biotinylated capture probes (anchored to a solid substrate via streptavidin) were then exposed to sample lysates. After 18S ribosomal ribonucleic acid (rRNA) target annealing, detection is mediated by digoxigenin (dig) labeled signal probes. The latter anneal to conserved regions of target molecules and bind anti-dig conjugate labeled horseradish peroxidase. The complex is then exposed to a substrate that produces either color or light. For ESP microarray assays, capture probes were resuspended in print buffer (0.1 M Tris HCl, 0.003 M EDTA, 0.497 M NaCl) and microarrays were printed on Optitran BA-S 83 reinforced nitrocellulose membranes (Whatman Inc., Dassel, Germany) with a Piezorray printing robot (Perkin-Elmer, Shelton, Connecticut). Capture probe storage, quantification and working concentrations were as previously reported (Jones et al., 2008).

All capture probes were tested against pure cultures of the podopleans, *Tisbe* sp. and *Tigriopus californicus*, and the calanoids, *Acartia* sp. and *Pseudodiaptomus* sp., obtained from Essential Live Feeds (Seattle, Washington). The copepods were fed pure cultures of *Isochrysis* sp. and *Nannochloropsis* sp. (from the same source). Calibration of copepod signals was conducted with individual copepods pipetted onto 5 μm Durapore PVDF 25 mm disc filters (Millipore) under gentle vacuum (< 10 mm Hg) and enumerated with an Olympus Research Stereo dissecting scope (SZH10) at 10–20× magnification. Developmental differences (e.g., body size, egg sacs presence or absence) were ignored for individuals used in dosage–response probe calibration tests; only the numbers of assayed individuals were recorded. Filters were frozen and stored in liquid nitrogen prior to SHA analysis. All other probes were designed to exclude these cultured copepod species, and they were tested against the pure cultures. Live *Mytilus galloprovincialis* veligers (Taylor Shellfish Hatchery, Quilcene, Washington) were used as a positive control for the previously designed mussel probe M2B and as a negative control for all other probes. Previously published probes were tested against extracts from frozen larvae, adult tissues, tow-net and whole water samples (see Goffredi et al., 2006; Jones et al., 2008).

3. Results

3.1. Calibration of new copepod probes

Taxon-specificities of the newly developed copepod probes were consistent with our expectations from the probe designs (Table 2). For example, Pod1951 detected the positive podoplean controls, *Tigriopus* and *Tisbe*, and discriminated against the negative calanoid controls, *Acartia* and *Pseudodiaptomus* (Fig. 2A,B). Pod1951 responded equally to positive controls regardless of the presence of negative controls. This sensitive probe could detect single individuals of *Tigriopus* or *Tisbe*, and dosage–response curves were essentially linear with respect to the number of target individuals (Fig. 3A,B). Detection at the A450 nm wavelength was nearly twice as sensitive as detection at A650 nm. The unicellular feed-algae *Isochrysis* and *Nannochloropsis* also were present in the test cultures. Culture-water replete with the feed-algae and devoid of copepods did not react with the targeted probes. Barnacle, mussel, polychaete and *C. maenas*-specific probes functioned as previously described (Jones et al., 2008) when tested against available control materials.

3.2. AUV/Gulper samples

Nine AUV/Gulper surveys returned 62 seawater samples (Table 1) and associated environmental data. Copepods comprised the most abundant fraction of zooplankton detected. One or more of the copepod probes detected targets in all 62 samples. Invertebrate larvae were less frequently detected. Of those, barnacle and mussel larvae were most frequently encountered, whereas polychaete and brachyuran larvae were less frequent. Zooplankton signals varied with physical, chemical and biological attributes of the associated water samples. For example, the 25 March survey (Table 1) sampled distinct water types (shelf water vs. recently upwelled water over the canyon) and the frontal zones near the shelf breaks (Fig. 1A,C). Greater zooplankton diversity and abundances occurred in shelf waters that were warmer, more nutrient depleted, and higher in chlorophyll. Cold nutrient-rich water, low in chlorophyll, characterized the upwelling filament between 35 and 60 km of this transect. Zooplankton abundance was lowest in the core of this upwelling filament (Fig. 1B, sample 5). Greatest calanoid copepod abundances occurred in the frontal zones that bounded the upwelling filament (Fig. 1B, samples 3 and 7).

Consistent with the synoptic example (Fig. 1), the full AUV data set exhibited clear relationships between environmental conditions and zooplankton abundance. For example, the greatest signal intensities (> 1.0 OD at A450 nm) for the Cal1939 calanoid probe occurred mainly in high chlorophyll waters with relatively high salinity, but across a range of water temperatures (Fig. 4A). Lower signal intensity was associated with recently upwelled waters that were low in temperature, oxygen, chlorophyll, and optical backscattering (a proxy for particle concentration), and high in salinity and nitrate. Principal components analysis (PCA) of all the environmental variables distributed AUV samples along vectors of comparable magnitude (Fig. 5A,B). Loadings (amount of variance attributed to each principal component) were as

Table 2
Capture probe design for sandwich hybridization assays. The 18S rRNA sequences considered in probe designs are listed with their respective taxa and associated GenBank accession numbers. The bold type denotes the capture probe, and the remaining sequences represent non-targeted sequences. Dots (.) represent nucleotides identical to probe sequence, and dashes (—) signify nucleotide deletions.

Probe	Order	Sequence	Source (Genbank accession numbers)
Cal903	Calanoida	**GCA CGA ATA TTC AGG CGT A–A**	(AF367719, AF514339–AF514344, AY335855–AY335857, AY335860, AY335861, AY446898, DQ839259, L81939)
		... ... .C. .-.	*Pseudocyclops* sp. (AY626994)
		... ... .G. ... .A. ... GT.	*Pseudocalanus* sp. (EU590909)
		... ... .A. ... GG-	*Arctodiaptomus dorsalis* (AY339147)
		... ... .A. ... G-.	*Eudiaptomus graciloides* (AY339149)
		... ... .A. ... .-.	*Skistodiaptomus oregonensis* (AY339159)
		... ... .A. .C- .TC	*Tortanus* sp. (AY626995)
		... ... .A. .A- .TC	*Candacia armata* (AY446899)
		... .A. C.. ... C.A .T- G-G	*Acartia tonsa* (FJ422281)
	Cyclopoida	... ... GT.	*Eucyclops speratus* (AJ746333)
		... ... GTC	*Macrocyclops albidus* (AJ746334)
		... ... G.. ... ... .TG	*Lamproglena chinensis* (DQ107553)
	Harpacticoida	... ... .G. ... .A. ... GT.	*Tigriopus californicus* (AF363306, AY588133)
		... .AG ... ... .A. ... GT.	*Euterpina acutifrons* (AY446896)
	Poecilostomatoida	... ... .A. ... GT.	*Ergasilus yaluzangbus* (DQ107578)
		... ... .A. ... TT.	*Lernentoma asellina* (AY627003)
		... ... .A. ... TT.	*Chondracanthus lophii* (L34046)
	Siphonostomatoida	... .CG ... ... .A. .T. .T.	*Dinemoura latifolia* (DQ538501)
		... .CG ... ... .A. .T. GT.	*Hatschekia* sp. (DQ538507)
		... ... .A. .T. GT.	*Aphotopontius mammillatus* (DQ538508)
	Monstrilloida	... .A. ... ... .A. ... .TC	*Monstrilla* spp. (DQ538496, DQ538495)
	Oribatida	... AC. T.. ... G.. .T- G-.	*Liodes* sp. (AF022035)
Cal1939	Calanoida	**ACA GTT TGG TCG TCT TCC CGC CAG**	(L81939, AF367719, AF514339-AF514344)
		CA.	*Pseudocyclops* sp. (AY626994)
		... ... .T. .A. T..	*Arctodiaptomus dorsalis* (AY339147)
		... ... .T. .A. T..	*Eudiaptomus graciloides* (AY339149)
		... ... .T. .A. ...	*Skistodiaptomus oregonensis* (AY339159)
		... ... C.. ... .T ..T .G.	*Tortanus* sp. (AY626995)
		... .A AGC A.. ..A A.- —	*Acartia tonsa* (FJ422281)
	Cyclopoida	CA. ... ... GA. ... .G GCA	*Eucyclops speratus* (AJ746333)
		CA. ... ... GAA ... .G GCA	*Macrocyclops albidus* (AJ746334)
		CA. ... C.. GAA ... ... .AG GCA	*Lamproglena chinensis* (DQ107553)
	Harpacticoida	CA. ... ... GA. ... ..T .AG -A	*Tigriopus californicus* (AF363306)
		CA. ... ... GA. ... — — —	*Euterpina acutifrons* (AY446912)
	Poecilostomatoida	CA. ... ... GA. ... — -AG -A	*Ergasilus yaluzangbus* (DQ107578)
		CA. ... ... GA. ... .T. .AG T.A	*Lernentoma asellina* (AY627003)
		CA. ... ... GA. ... .T. .AG T.A	*Chondracanthus lophii* (L34046)
	Siphonostomatoida	CA. ... ... GA. ... ..T .AA -A	*Dinemoura latifolia* (DQ538501)
		CA. ... ... GA. ... .TT ..A -A	*Hatschekia* sp. (DQ538507)
		CA. ... ... GA. ... ..T ..G -A	*Aphotopontius mammillatus* (DQ538508)
	Monstrilloida	CA. ... ... GA. ... .TT .AA .-A	*Monstrilla clavata* (DQ538495)
		CA. ... ..A .A. ... ..T .AA .GC	*Monstrilla* sp. (DQ538496)
	Oribatida	CA. ... ... G.A ... .T. .AA ACA	*Liodes* sp. (AF022035)
Pod1951	Podoplea	**ACG CTC AAG TTT GGG AGT CT**	(AF363306, AY446912, DQ107578, AY627003, L34046, DQ538501, DQ538507, DQ538508, AJ746333)
	Cyclopoida	... ... .A. ..	*Macrocyclops albidus* (AJ746334)
		... ...C ... .A. ..	*Lamproglena chinensis* (DQ107553)
	Monstrilloida	.T.	*Monstrilla clavata* (DQ538495)
		.T. ... ... .AT	*Monstrilla* sp. (DQ538496)
	Oribatida	.T. .T. ... ... CA. ..	*Liodes* sp. (AF022035)
	Calanoida	.T. ... ...T C.. ..	*Pseudocyclops* sp. (AY626994)
		G.. ..A C.. ... ..T C.. ..	*Arctodiaptomus dorsalis* (AY339147)
		G.. ..A C.. ... ..T C.. ..	*Eudiaptomus graciloides* (AY339149)
		G.. ..A C.. ... ..T C.. ..	*Skistodiaptomus oregonensis* (AY339159)
		GT. ..A C.. ..C ..T C.. ..	*Tortanus* sp. (AY626995)
		... ..A C.. ... ..T C.. ..	*Calanus pacificus* (L81939)
		... ..A C.. ... ..T C.. ..	*Calanus finmarchicus* (AF367719)
		... ..A C.. ... ..T C.. ..	*Neocalanus cristatus* (AF514341-AF514344)
		... ..A C.. ... ..T C.. ..	*Neocalanus flemingeri* (AF514339)
		... ..A C.. ... ..T C.. ..	*Neocalanus plumchrus* (AF514340)
		.T. AA. G.. ..C .C. CA. ..	*Derocheilocaris typicus* (L81937)
		-. ACA C.. ... .AA GCA ..	*Acartia tonsa* (FJ422281)
Crab903	Brachyura	**ATG CAT AGG CAT TCA GGC CGT**	(AY743951, EU284152, DQ079744, AY527220, DQ079743, DQ079763, AY216710)
	Arguloida	... ..C CAT T.. ..T ... .A.	*Argulus nobilis* (M27187)
	Mystacocaridida	... ..A CAA T.. ..T ... -A.	*Derocheilocaris typicus* (L81937)
	Decapoda	... ..C GAC ... ..G ... T..	*Penaeus vannamei* (AF186250)
		... ... .TC	*Eucrate crenata* (EU284154)
		... ... A.. AA. A..	*Xantho poressa* (FM161989)
		GA. .CC .A. TC. .TT ... T..	*Dorippoides facchino* (DQ925829)
		GA. .CC .A. TC. .TT ... T..	*Carpilius convexus* (DQ925834)
		GA. .CC .A. TC. .TT ... T..	*Daira perlata* (DQ925835)
		GA. .CC .A. TC. .TT ... T..	*Calappa bilineata* (DQ925838)
		GA. .CC .A. TC. .TT ... T..	*Aethra scruposa* (DQ925839)
		GA. .CC .A. TC. .TT ... T..	*Menaethius monoceros* (DQ925841)

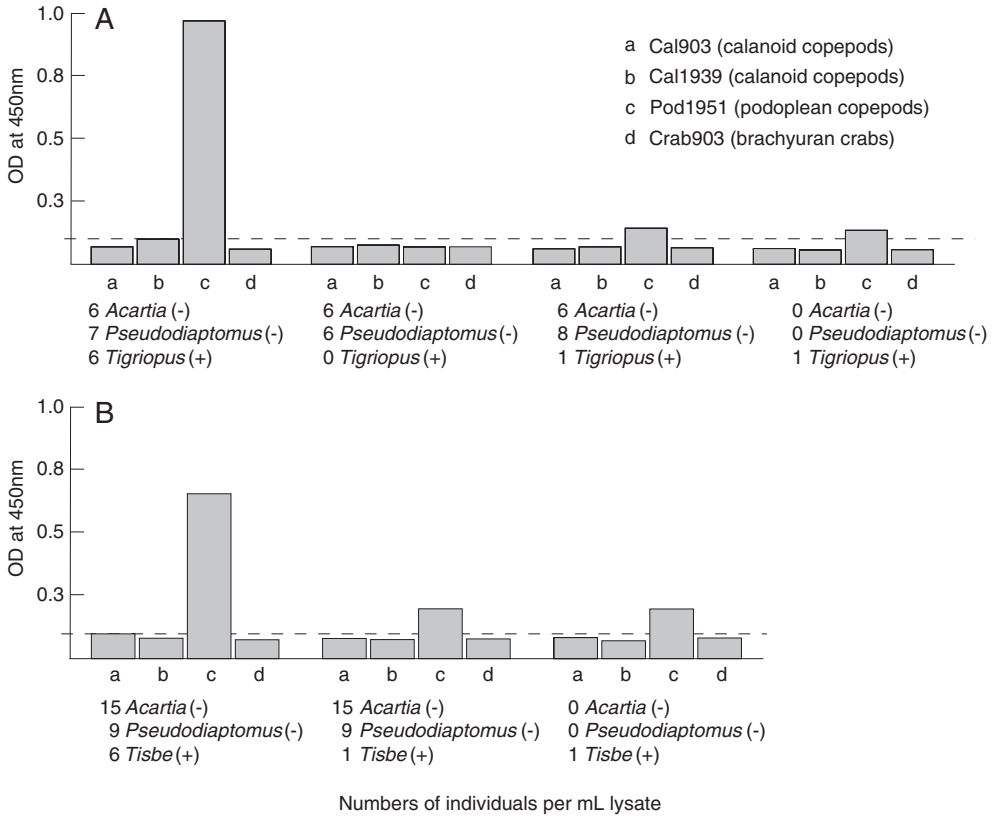

Fig. 2. Testing of four new SHA capture probes against four copepod species from pure cultures. *Tigriopus californicus* and *Tisbe* sp. served as positive control targets for podoplean copepod capture probe Pod1951 only. (A) Varying numbers of *Tigriopus californicus* individuals mixed with varying numbers of *Acartia* and *Pseudodiaptomus*. (B) Variable numbers of *Tisbe* sp. individuals were mixed with varying numbers of *Acartia* and *Pseudodiaptomus*. Dashed line represents the lower detection limit. Numbers of Pod1951 target (+) and non-target (−) species in each trial are indicated.

follows: PC1 = 56.7%; PC2 = 21.8%; PC3 = 11.6%; PC4 = 5.4%; and PC5 = 3.2%. PC1 through 3 accounted for over 90% of the cumulative variance. As indicated by the directionality of environmental variable vectors (Fig. 5B), PC1 primarily reflected variation in chlorophyll; optical backscatter; oxygen and nitrate and PC2 most strongly represented variation in temperature and salinity values. Warm, low salinity, low nitrate samples with moderate to high chlorophyll frequently contained the greatest diversity and abundances of copepods and larvae (Fig. 5E,F). Cold, high salinity water samples with high nitrate and low chlorophyll concentrations had weak to nonexistent biological signals (Fig. 5C). The strongest calanoid signals (from capture probe Cal1939) were associated with cold, high salinity, low nitrate, high chlorophyll, and high backscatter waters (Fig. 5D).

3.3. ESP samples

Three ESP deployments during 2009 generated 14 seawater samples (Fig. 6). The spring deployment (20–22 April), conducted at an average depth of 9 m, was associated with lower temperatures and higher salinity relative to the shallower fall deployments (average depth 7 m). Maximum chlorophyll concentrations during the spring deployment were nearly twice the maximum values during the fall

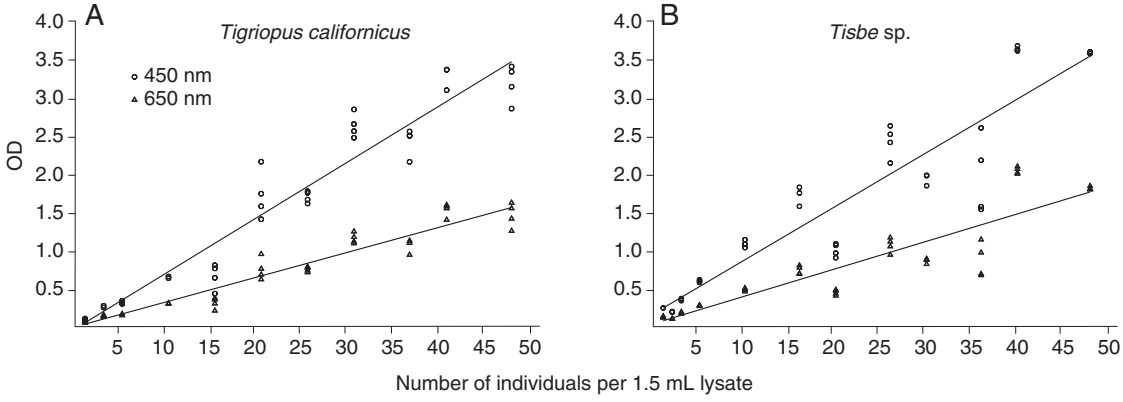

Fig. 3. SHA dosage–response curves for Pod1951 probe against: (A) *Tigriopus californicus* individuals (A_{450} nm wavelength measurement trend-line: $y = 0.0747x - 0.0284$, $R^2 = 0.9447$; A_{650} nm wavelength measurement trend-line: $y = 0.0333x - 0.0048$, $R^2 = 0.9399$), and (B) *Tisbe* sp. individuals (A_{450} nm wavelength measurement trend-line: $y = 0.0704x + 0.1742$, $R^2 = 0.8742$; A_{650} nm wavelength measurement trend-line: $y = 0.036x + 0.0416$, $R^2 = 0.8246$).

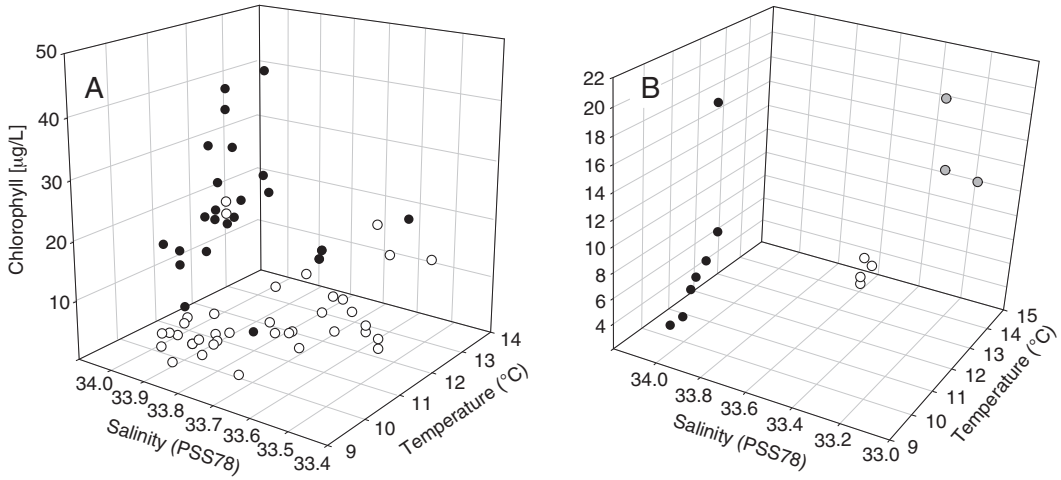

Fig. 4. Plots of temperature, salinity and chlorophyll associated with water samples. (A) AUV/Gulper samples ($n=62$). Black dots indicate SHA detection signals > 1.0 OD at A450 nm for probe Cal1939, whereas white dots indicate signals < 1.0 OD. (B) ESP samples ($n=14$). Black dots indicate microarray fluorescence (Cal1939) > 10,000 counts, gray dots are < 10,000, and white dots indicate no signal.

deployments. Overall, the range of spring chlorophyll concentrations was at least two times greater than the range during the fall.

The strongest zooplankton signals from these samples were obtained with the Euk338 (eukaryotic general) and Cal1939 (calanoid) probes (Fig. 7). Cal1939 signals were strongest during the spring and weak to negligible during the fall. The strongest calanoid signals were associated with lower temperatures and higher salinities (Fig. 6, samples 1–7) in the presence of chlorophyll (Fig. 4B, black dots). Weaker calanoid signals occurred at higher temperatures and low salinity conditions in the three Fall-2 samples (Fig. 4B, gray dots). Though the Fall-1 samples returned no Cal1939 signals (Fig. 4B, white dots), these samples provided the highest diversity of relatively weak signals for other copepods and for invertebrate larvae. The associated environmental conditions were moderate to warm temperatures, intermediate salinity levels, and intermediate to low chlorophyll concentrations (Fig. 6).

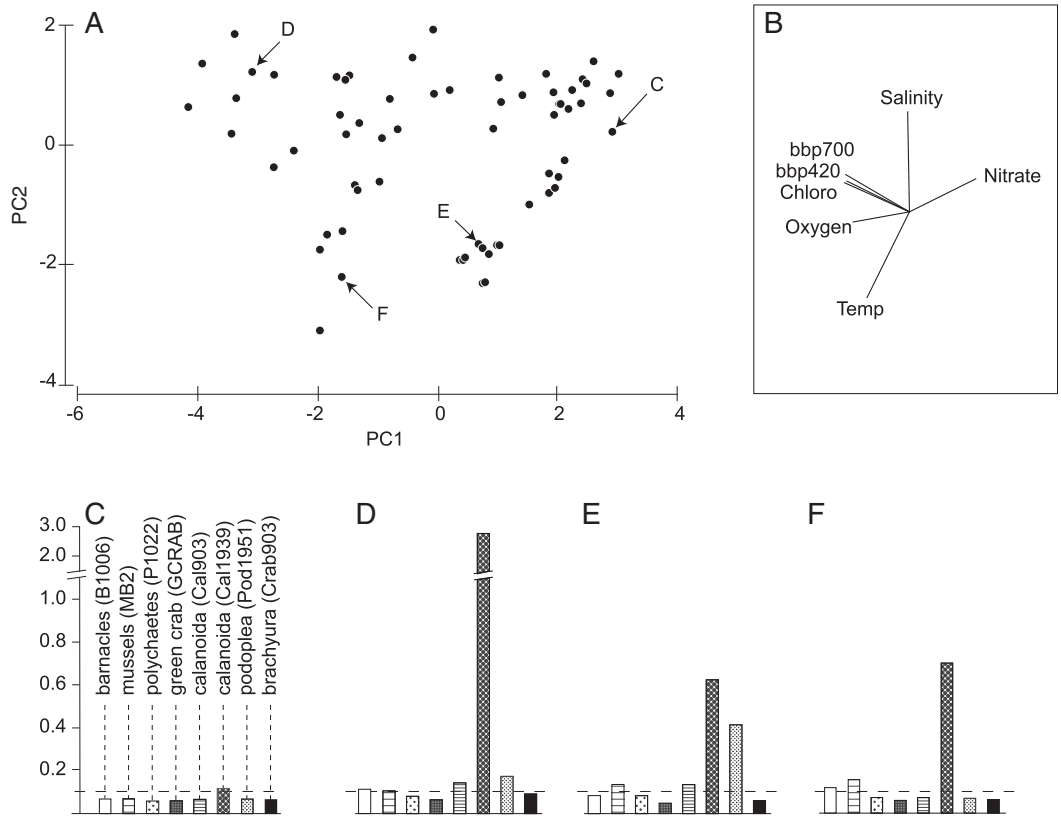

Fig. 5. AUV/Gulper samples. (A) Principal components analysis of environmental variables. (B) Vectors for the environmental variables. Chloro = fluorometric chlorophyll-a concentration, bbp = optical backscatter at 420 and 700 nm, respectively. (C–F) Samples corresponding with following histograms of SHA probe signal intensities. Dashed lines indicate lower detection limit.

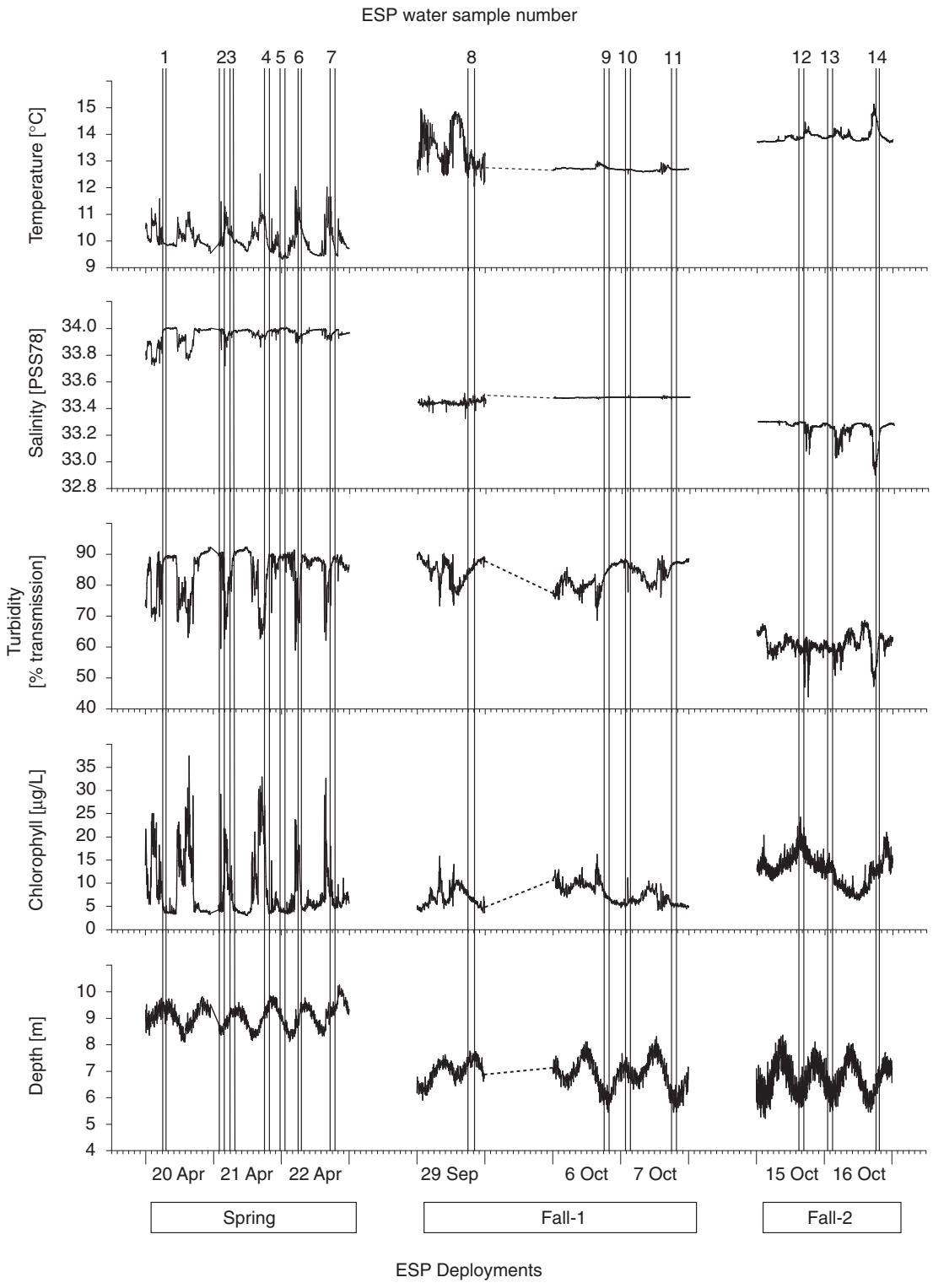

Fig. 6. ESP environmental data. Vertical lines denote sample collection durations (1–2 h). The break in environmental data collection (dashed line) during the Fall-1 deployment reflects an unrelated sampling effort aimed at marine bacteria.

4. Discussion

4.1. Summary

(1) The present combination of molecular probes and robotic sampling at a sufficiently high resolution to capture patchy variation, assessed zooplankton diversity and relative abundance associated with environmental covariates in Monterey Bay, California. Zooplankton diversity and abundance were greater in shelf waters relative to recently upwelled waters. Calanoid copepods were generally associated with elevated chlorophyll, as has been found by other researchers investigating copepods (Morales et al., 2010; Papastephanou et al., 2006), larger zooplankton (e.g. euphausiids, Ressler et al., 2005), and zooplanktivourous salmon (Bi et al., 2008). However, beyond the expected relationship between chlorophyll and higher trophic levels sustained by primary productivity, high-

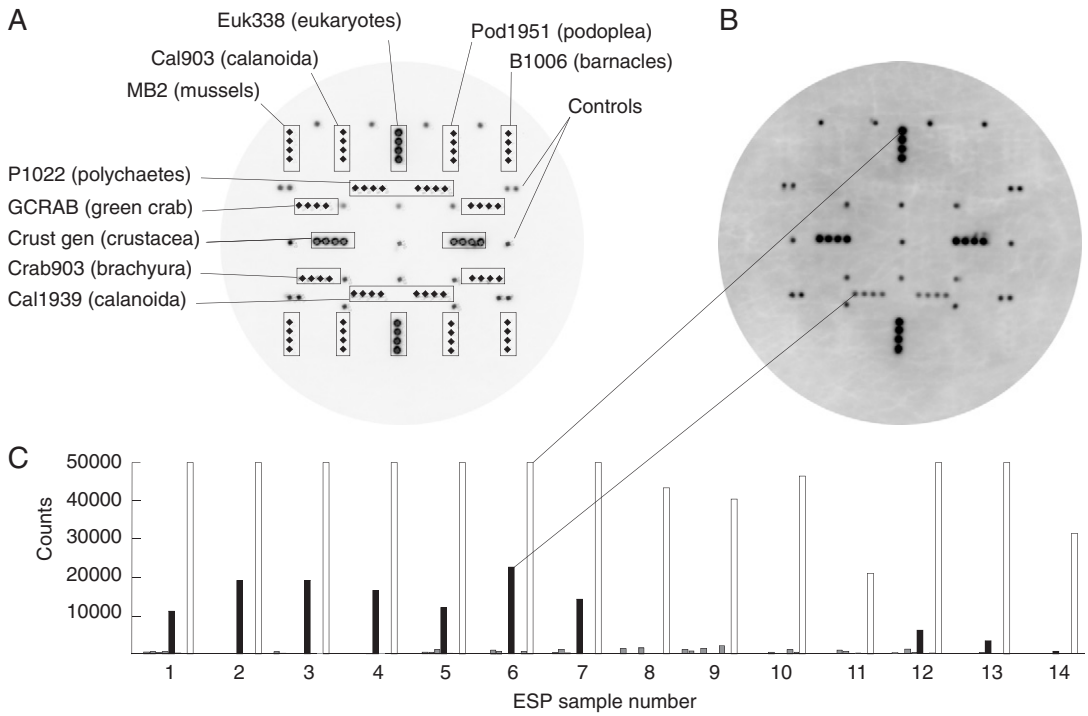

Fig. 7. ESP microarray results. (A) Map of probe locations. Boxes surround groups of replicate probes. Each group is symmetrically paired. Single and double spots are internal controls and aid in orientation. (B) Microarray result for ESP sample 6. Cal1939 (calanoida) and Euk338 (eukaryote) signals are linked to corresponding bars on histogram of microarray results for $n = 14$ samples (C).

resolution sampling revealed that calanoid copepods were most abundant at the margins of upwelling fronts where physical, chemical and biological gradients were enhanced. (2) Despite very different water-sampling and molecular methods implementation, both the AUV and ESP returned corroborative data supporting similar conclusions. (3) Upwelling fronts appear to concentrate copepods and other zooplankton (e.g., Roughgarden et al., 1991), making these features excellent candidates for fine-scale, adaptive sampling efforts aimed at understanding zooplankton population dynamics.

4.2. Environmental correlates of zooplankton abundance

The AUV/Gulper samples were taken during a period (March–June) associated with seasonal changes in the California Current system, including an increase in wind-driven upwelling and primary productivity (Collins et al., 2003; Lynn et al., 2003). Our results revealed relationships between spatial hydrographic variation and the relative abundance of zooplankton, exemplified by one synoptic AUV survey (Fig. 1). Greater zooplankton abundance characterized shelf water samples with moderate to warm temperatures, low nitrate and high chlorophyll concentrations. In contrast, low to negligible abundance occurred in recently upwelled waters characterized by low temperatures, low chlorophyll and high nitrate concentrations. Patterns in sea-surface temperature (Fig. 1A,C) confirmed transit of the vehicle across an upwelling filament that originated north of Monterey Bay. Frontal zones between these cold, recently upwelled waters and warmer, surface waters over the shelf contained the greatest abundance of calanoid copepods. Possible explanations for this pattern include physical aggregation that can occur through the interaction of ocean currents and plankton motility (Roughgarden et al., 1991) and biological influences such as favorable growth conditions within dynamic frontal zones at the margins of highly productive shelf waters. Upwelling filaments were previously noted to affect the biomass and species-composition of copepod assemblages (Keister et al., 2009b; Papastephanou et al., 2006; Peterson and Keister, 2003). The frontal zones of upwelling filaments may, therefore, be key oceanographic features to monitor for zooplankton biodiversity and abundance.

Calanoid copepod abundance was clearly associated with elevated chlorophyll (Figs. 4A, 5). Samples that were cold and salty, yet low in nitrate and high in chlorophyll represent abundant food resources due to primary productivity fueled by recent upwelling. Elevated salinity is a signal of recent upwelling, and depletion of nitrate is a signal of biological drawdown of the nutrients supplied by that upwelling. The strong calanoid signals associated with these samples might represent increased grazer presence or simply aggregation due to physical forces. Processes occurring at multiple scales may govern zooplankton aggregation, however. At the larger scale of Monterey Bay, convergent flow in upwelling fronts can concentrate motile zooplankton (Roughgarden et al., 1991). At smaller scales, swimming behavior may enhance aggregation of grazers in phytoplankton patches. Prior to upwelling, cold, salty, high nitrate, low oxygen waters yield low to negligible zooplankton abundance (Fig. 5C). Calanoid copepods are abundant at upwelling fronts, where water is still cold and salty but nitrate drops and chlorophyll increases with primary productivity (Fig. 5D). As upwelled waters warm, freshen and mix with shelf waters, primary production and zooplankton species richness increase over time (Fig. 5E,F). Zooplankton abundance was unrelated to location (depth, latitude and longitude) in the present samples. Taxonomically lower-level probes and finer-scale sampling of the environment might reveal more subtle location effects. Nonetheless, taxonomically fine-scale probes for some of the invertebrate larvae also failed to detect location effects.

In contrast to the spring AUV samples, ESP samples were collected during both spring and fall. Nonetheless, ESP samples also revealed an association between calanoid copepod abundance and cold, high salinity water with elevated chlorophyll (Fig. 4B). Calanoids were detected during the Spring and Fall-2 deployments (Fig. 7C), characterized by relatively high chlorophyll levels (Fig. 6). Calanoid abundance was greatest during the spring, coinciding with low temperature, high salinity conditions indicative of strong upwelling. Highly variable chlorophyll concentrations during the spring provide

evidence that phytoplankton patches advected past the ESP or that tidal changes moved the ESP in and out of stratified phytoplankton patches. Conversely, low chlorophyll concentrations and an absence of calanoid copepods occurred during the Fall-1 deployment. Annual upwelling maxima are typically associated with the spring–summer period in the Monterey Bay (Pennington and Chavez, 2000). Beyond seasonal considerations, ESP sampling results are probably influenced by differences among deployment bottom depths and locations. Upwelling circulation that originates from north of the Monterey Bay engenders formation of an upwelling shadow in the northern bay, which influences the dispersal and diversity of zooplankton assemblages (Graham and Largier, 1997; Graham et al., 1992). The Fall ESP deployments were inside the upwelling shadow and sheltered from direct wind forcing and upwelling filaments. In contrast, the Spring deployment was further south and more likely to be in the direct path of upwelling filaments.

4.3. Methodological considerations

We employed two water-sampling strategies. Sample volumes were small, relative to traditional methods such as tow netting; consequently, organisms present in low abundance may not have been collected. If the sampling results were very sparse, one would expect to see a random, Poisson-distributed, data set with many zeros. Instead, our molecular detection methods consistently revealed the presence of targeted organisms in samples obtained with both platforms. The mobile AUV/Gulper system sampled over space whereas the stationary ESP systems sampled three individual locations over time; however, other differences also exist. Mechanical differences between these platforms may have biased sample contents. The AUV system "gulps" ~1.8 L of water within 1–2 s, whereas the ESP system "sips" ≤4 L of water during a 1–2-hour interval. Slowly sipping water might allow active avoidance by larger zooplankton with strong swimming abilities. Furthermore, the sensitivity of target detection differed between these systems. The ex situ SHA methods used with AUV samples were more sensitive than the in situ microarray assays used with ESP samples. Nonetheless, both the AUV and ESP results corresponded in identifying relationships between copepod abundance and environmental conditions associated with upwelling.

Previous molecular studies developed taxonomically fine-scale genetic probes or PCR primers to identify various species, genera or families of primary interest (Deagle et al., 2003; Harvey et al., 2009; Jones et al., 2008). Fine-scale approaches are potentially very sensitive, but they will not identify the presence of non-target taxa. In contrast, our SHA methods were designed to work hierarchically, starting first with probes that identify Eukaryotes and progressing to probes that distinguished invertebrate phyla and orders. This broad-scale approach offers a robust preliminary characterization of environmental correlates of zooplankton diversity, but it risks confounding the diversity and abundance of lower-level taxa in genetically diverse zooplankton samples. The present SHA methods relied on high copy-number ribosomal RNA targets. These slowly evolving genes are taxonomically conservative, thereby limiting finer resolution below the family level for most taxa. To determine the diversity and abundance of lower-level taxa, analyses of genes displaying greater variability are required. The AUV/Gulper returns multiple samples to shore, while the ESP supports both onboard sample preservation and in situ qPCR assays (e.g., Ottesen et al., 2011; Preston et al., 2011). In both cases, further sample analysis by subsequent gene amplification, cloning and sequencing of more variable genes with the potential to resolve lower-level taxa is possible. Resulting sequence data could then be used to develop probes with progressively finer taxonomic resolution.

Relating SHA signal quantitation to organismal abundance requires further investigation. Dosage–response curves for Pod1951's positive control targets were remarkably linear and similar to results previously obtained for SHA detection of barnacle and mussel larvae (Goffredi et al., 2006; Jones et al., 2008). The dosage–response signals clearly corresponded with the number of invertebrate larvae up to a point of probe saturation. Lower limits for detection of *Tigriopus* and *Tisbe* by Pod1951 were single individuals, possibly due to larger copepod body sizes relative to the invertebrate larvae that were previously tested. Nevertheless, SHA methods estimate total rRNA concentration, which is confounded by ontogenic changes, body size variation, gravidity, and rRNA degradation. Species-specific differences will also affect relationships between individual numbers and signal strength (Jones et al., 2008). Also, SHA detection cannot differentiate between living individuals and their remnants in the gut contents or feces of planktonic predators. Calibration curves might be improved through quantification of target biomass rather than individual numbers (Baguley et al., 2004). To assess their precision, calibration curves for specific targets should be re-investigated in mixed cultures involving a more natural diversity of zooplankton taxa.

4.4. Future efforts

Particular zooplankton taxa critical to the health and productivity of a region should be characterized to provide a baseline for monitoring of seasonal and longer-term environmental changes. Such efforts will require the development of molecular probes with finer taxonomic resolution along with concurrent morphological verifications. The ESP is currently capable of archiving samples for subsequent morphological analyses, and AUV/Gulper samples can be partitioned for molecular and morphological analyses. To more precisely assess spatial and temporal dynamics of oceanographic features such as upwelling fronts, adaptive sampling approaches for the AUV/Gulper and ESP platforms are under development at MBARI (McGann et al., 2008; Rajan et al., 2009; Zhang et al., 2010). Adaptive approaches use artificial intelligence to track and sample features defined by specific environmental parameters (Ryan et al., 2010). Oceanographers are now in a unique position to develop platforms capable of observing ocean systems in novel ways, including molecular detection of native zooplankton and invasive species (Jones et al., 2008). This work comprises one component of multi-disciplinary efforts to test ecological and evolutionary hypotheses and develop continuous monitoring capabilities for the Monterey National Marine Sanctuary.

Acknowledgements

Funding provided by the Packard Foundation and the National Science Foundation (NSF OCE-0314222 to C. A. Scholin). Many thanks to MBARI's AUV and ESP engineering teams (H. Thomas, D. Conlin, D. Thompson, J. Birch, B. Roman, S. Jensen, D. Pargett), the crew of the R/V *Zephyr*, M. McCann (MBARI), S. Wilson (MBARI), A. Rhodes (Essential Live Feeds) and B. Eudeline (Taylor Shellfish).

References

Baguley, J.G., Hyde, L.J., Montagna, P.A., 2004. A semi-automated digital microphotographic approach to measure meiofaunal biomass. Limnol. Oceanogr. Methods 2, 181–190.

Bi, H.S., Ruppel, R.E., Peterson, W.T., Casillas, E., 2008. Spatial distribution of ocean habitat of yearling Chinook (*Oncorhynchus tshawytscha*) and Coho (*Oncorhynchus kisutch*) salmon off Washington and Oregon, USA. Fish. Oceanogr. 17, 463–476.

Bird, L.E., Sherman, A.D., Ryan, J.P., 2007. Development of an active, large volume, discrete seawater sampler for autonomous underwater vehicles. Proceedings of the Oceans MTS/IEEE Conference, Vancouver, Canada.

Bucklin, A., Frost, B.W., Kocher, T.D., 1995. Molecular systematics of six *Calanus* and three *Metridia* species (Calanoida: Copepoda). Mar. Biol. 121, 655–664.

Collins, C.A., Pennington, J.T., Castro, C.G., Rago, T.A., Chavez, F.P., 2003. The California Current system off Monterey, California: physical and biological coupling. Deep-Sea Res. Part II 50, 2389–2404.

Darling, J.A., Blum, M.J., 2007. DNA-based methods for monitoring invasive species: a review and prospectus. Biol. Invasions 9, 751–765.

Deagle, B.E., Bax, N.J., Hewitt, C.L., Patil, J.G., 2003. Development and evaluation of a PCR-based test for detection of *Asterias* (Echinodermata: Asteroidea) larvae in Australian plankton samples from ballast water. Mar. Freshw. Res. 54, 709–719.
Garland, E.D., Zimmer, C.A., 2002. Techniques for the identification of bivalve larvae. Mar. Ecol. Prog. Ser. 225, 299–310.
Goffredi, S.K., Jones, W.J., Scholin, C.A., Marin, R., Vrijenhoek, R.C., 2006. Molecular detection of marine invertebrate larvae. Mar. Biotechnol. 8, 149–160.
Graham, W.M., Largier, J.L., 1997. Upwelling shadows as nearshore retention sites: the example of northern Monterey Bay. Cont. Shelf Res. 17, 509–532.
Graham, W.M., Field, J.G., Potts, D.C., 1992. Persistent upwelling shadows and their influence on zooplankton distributions. Mar. Biol. 114, 561–570.
Greenfield, D.I., Marin, R., Jensen, S., Massion, E., Roman, B., Feldman, J., Scholin, C.A., 2006. Application of environmental sample processor (ESP) methodology for quantifying *Pseudo-nitzschia australis* using ribosomal RNA-targeted probes in sandwich and fluorescent *in situ* hybridization formats. Limnol. Oceanogr. Methods 4, 426–435.
Greenfield, D.I., Marin, R., Doucette, G.J., Mikulski, C., Jones, K., Jensen, S., Roman, B., Alvarado, N., Feldman, J., Scholin, C., 2008. Field applications of the second-generation Environmental Sample Processor (ESP) for remote detection of harmful algae: 2006–2007. Limnol. Oceanogr. Methods 6, 667–679.
Harvey, J.B.J., Hoy, M.S., Rodriguez, R.J., 2009. Molecular detection of native and invasive marine invertebrate larvae present in ballast and open water environmental samples collected in Puget Sound. J. Exp. Mar. Biol. Ecol. 369, 93–99.
Haywood, A.J., Scholin, C.A., Marin, R., Steidinger, K.A., Heil, C., Ray, J., 2007. Molecular detection of the brevetoxin-producing dinoflagellate *Karenia brevis* and closely related species using rRNA-targeted probes and a semiautomated sandwich hybridization assay. J. Phycol. 43, 1271–1286.
Hutchinson, G.E., 1961. The paradox of the plankton. Am. Nat. 95, 137–145.
Jones, W.J., Preston, C.M., Marin, R., Scholin, C.A., Vrijenhoek, R.C., 2008. A robotic molecular method for *in situ* detection of marine invertebrate larvae. Mol. Ecol. Resour. 8, 540–550.
Keister, J.E., Peterson, W.T., Pierce, S.D., 2009a. Zooplankton distribution and cross-shelf transfer of carbon in an area of complex mesoscale circulation in the northern California Current. Deep-Sea Res. Part I 56, 212–231.
Keister, J.E., Cowles, T.J., Peterson, W.T., Morgan, C.A., 2009b. Do upwelling filaments result in predictable biological distributions in coastal upwelling ecosystems? Prog. Oceanogr. 83, 303–313.
Lynn, R.J., Bograd, S.J., Chereskin, T.K., Huyer, A., 2003. Seasonal renewal of the California Current: the spring transition off California. J. Geophys. Res. Oceans 108, 1–11.
Mackas, D.L., Beaugrand, G., 2010. Comparisons of zooplankton time series. J. Mar. Syst. 79, 286–304.
McClatchie, S., Goericke, R., Koslow, J.A., Schwing, F.B., Bograd, S.J., Charter, R., Lo, W.W.N., Hill, K., Gottschalck, J., L'Heureux, M., Xue, Y., Peterson, W.T., Emmett, R., Collins, C., Gaxiola-Castro, G., Durazo, R., Kahru, M., Mitchell, B.G., Hyrenbach, K.D., Sydeman, W.J., Bradley, R.W., Warzybok, P., Bjorkstedt, E., 2008. The state of the California Current, 2007–2008: La Nina conditions and their effects on the ecosystem. Calif. Coop. Ocean. Fish. Invest. Rep. 49, 39–76.
McGann, C., Py, F., Rajan, K., Thomas, H., Henthorn, R., McEwen, R., 2008. Preliminary results for model-based adaptive control of an autonomous underwater vehicle. 11th International Symposium on Experimental Robotics, Athens, Greece.
Morales, C.E., Torreblanca, M.L., Hormazabal, S., Correa-Ramirez, M., Nunez, S., Hidalgo, P., 2010. Mesoscale structure of copepod assemblages in the coastal transition zone and oceanic waters off central-southern Chile. Prog. Oceanogr. 84, 158–173.
Ottesen, E.A., Marin III, R., Preston, C.M., Young, C.R., Ryan, J.P., Scholin, C.A., DeLong, E.F., 2011. Metatranscriptomic analysis of autonomously collected and preserved marine bacterioplankton. ISME J. doi:10.1038/ismej.2011.70
Papastephanou, K.M., Bollens, S.M., Slaughter, A.M., 2006. Cross-shelf distribution of copepods and the role of event-scale winds in a northern California upwelling zone. Deep-Sea Res. Part II 53, 3078–3098.
Patil, J.G., Gunasekera, R.M., Deagle, B.E., Bax, N.J., 2005. Specific detection of Pacific oyster (*Crassostrea gigas*) larvae in plankton samples using nested polymerase chain reaction. Mar. Biotechnol. 7, 11–20.
Pennington, J.T., Chavez, F.P., 2000. Seasonal fluctuations of temperature, salinity, nitrate, chlorophyll and primary production at station H3/M1 over 1989–1996 in Monterey Bay, California. Deep-Sea Res. Part II 47, 947–973.
Peterson, W.T., Keister, J.E., 2003. Interannual variability in copepod community composition at a coastal station in the northern California Current: a multivariate approach. Deep-Sea Res. Part II 50, 2499–2517.
Preston, C.M., Marin, R., Jensen, S.D., Feldman, J., Birch, J.M., Massion, E.I., DeLong, E.F., Suzuki, M., Wheeler, K., Scholin, C.A., 2009. Near real-time, autonomous detection of marine bacterioplankton on a coastal mooring in Monterey Bay, California, using rRNA-targeted DNA probes. Environ. Microbiol. 11, 1168–1180.
Preston, C.M., Harris, A., Ryan, J.P., Roman, B., Marin III, R., Jensen, S., Everlove, C., Birch, J., Dzenitis, J.M., Pargett, D., Adachi, M., Turk, K., Zehr, J.P., Scholin, C.A., 2011. Underwater application of quantitative PCR on an ocean mooring. PLoS One 6, e22522. doi:10.1371/journal.pone.0022522.
Puig, P., Company, J.B., Sard, F., Palanques, A., 2001. Responses of deep-water shrimp populations to intermediate nepheloid layer detachments on the Northwestern Mediterranean continental margin. Deep-Sea Res. 48, 2195–2207.
Rajan, K., Py, F., McGann, C., Ryan, J., O'Reilly, T., Maughan, T., Roman, B., 2009. Onboard adaptive control of AUVs using automated planning and execution. Symposium on Unmanned Untethered Submersible Technology, Durham, New Hampshire, USA.
Rasband, W.S., 2008. ImageJ 1.41. U.S. National Institute of Health, Bethesda, Maryland, USA.
Reid, P.C., Colebrook, J.M., Matthews, J.B.L., Aikend, J., 2003. The continuous plankton recorder: concepts and history, from plankton indicator to undulating recorders. Prog. Oceanogr. 58, 117–173.
Ressler, P.H., Brodeur, R.D., Peterson, W.T., Pierce, S.D., Vance, P.M., Rostad, A., Barth, J.A., 2005. The spatial distribution of euphausiid aggregations in the Northern California Current during August 2000. Deep-Sea Res. Part II 52, 89–108.
Roman, B., Scholin, C., Jensen, S., Massion, E., Marin, R., Preston, C., Greenfield, D., Jones, W., Wheeler, K., 2007. Controlling a robotic marine environmental sampler with the ruby script language. J. Assoc. Lab. Auto. 12, 56–61.
Roughgarden, J., Pennington, J.T., Stoner, D., Alexander, S., Miller, K., 1991. Collisions of upwelling fronts with the intertidal zone—the cause of recruitment pulses in barnacle populations of central California. Acta Oecol. Int. J. Ecol. 12, 35–51.
Ryan, J.P., McManus, M.A., Paduan, J.D., Chavez, F.P., 2008. Phytoplankton thin layers caused by shear in frontal zones of a coastal upwelling system. Mar. Ecol. Prog. Ser. 354, 21–34.
Ryan, J.P., Johnson, S.B., Sherman, A., Rajan, K., Py, F., Thomas, H., Harvey, J.B.J., Bird, L., Paduan, J.D., Vrijenhoek, R.C., 2010. Mobile autonomous process sampling within coastal ocean observing systems. Limnol. Oceanogr. Methods 8, 394–402.
Scheltema, R.S., 1986. Long-distance dispersal by the planktonic larvae of shoal-water benthic invertebrates among central Pacific islands. Bull. Mar. Sci. 39, 241–256.
Schlining, B., 2009. ESP Image Analysis Application 1.0. Monterey Bay Aquarium Research Institute, Moss Landing, California, USA.
Scholin, C.A., Marin, R., Miller, P.E., Doucette, G.J., Powell, C.L., Haydock, P., Howard, J., Ray, J., 1999. DNA probes and a receptor-binding assay for detection of *Pseudo-nitzschia* (Bacillariophyceae) species and domoic acid activity in cultured and natural samples. J. Phycol. 35, 1356–1367.
Scholin, C., Doucette, G., Jensen, S., Roman, B., Pargett, D., Marin, R., Preston, C., Jones, W., Feldman, J., Everlove, C., Harris, A., Alvarado, N., Massion, E., Birch, J., Greenfield, D., Vrijenhoek, R., Mikulski, C., Jones, K., 2009. Remote detection of marine microbes, small invertebrates, harmful algae, and biotoxins using the environmental sample processor (ESP). Oceanography 22, 158–167.
Smith, K.F., Rhodes, L.L., Adamson, J.E., Tyrrell, J.V., Mountfort, D.O., Jones, W.J., 2011. Application of a sandwich hybridisation assay for rapid detection of the Northern Pacific seastar, *Asterias amurensis*. N. Z. J. Mar. Freshw. Res. 45, 145–152.
Stothard, P., 2000. The Sequence Manipulation Suite: JavaScript programs for analyzing and formatting protein and DNA sequences. Biotechniques 28, 1102–1104.
Thorson, G., 1950. Reproductive and larval ecology of marine bottom invertebrates. Biol. Rev. 25, 1–45.
Zhang, Y., McEwen, R.S., Ryan, J.P., Bellingham, J.G., 2010. Design and tests of an adaptive triggering method for capturing peak samples in a thin phytoplankton layer by an autonomous underwater vehicle. IEEE J. Ocean. Eng. 35, 785–796.